The Use of Cellulose Membrane to Eliminate Burst Release from Intravaginal Rings

Ignacio M. Helbling, Juan C. D. Ibarra & Julio A. Luna

The AAPS Journal
An Official Journal of the American Association of Pharmaceutical Scientists

e-ISSN 1550-7416
Volume 18
Number 4

AAPS J (2016) 18:960-971
DOI 10.1208/s12248-016-9914-1

Springer

The AAPS Journal, Vol. 18, No. 4, July 2016 (© 2016)
DOI: 10.1208/s12248-016-9914-1

Research Article

The Use of Cellulose Membrane to Eliminate Burst Release from Intravaginal Rings

Ignacio M. Helbling,[1,2] Juan C. D. Ibarra,[1] and Julio A. Luna[1]

Received 2 February 2016; accepted 6 April 2016; published online 20 April 2016

Abstract. Burst release was observed when ethylene vinyl acetate copolymer (EVA) intravaginal rings were tested for progesterone release in our previous work (Helbling *et al.* Pharm Res. 31(3):795–808, 2014). Burst release is undesirable in controlled delivery devices because release is uncontrollable and higher levels of active pharmaceutical ingredient could lead to the occurrence of adverse effect. The present contribution is about the use of membranes to coat EVA rings to eliminate burst release. Physicochemical state of progesterone in uncoated rings and the solubility and diffusion coefficient in membrane were studied. Hormone delivery from several rings of different sizes was compared. A mathematical model was used to analyze the effects of membrane properties on delivery rate. No chemical interactions were detected between hormone and polymer. Hormone was mainly forming amorphous aggregates inside rings, and migration to membrane was not observed during storage. Diffusion coefficient was smaller in membrane ($\sim 10^{-8}$ cm^2 s^{-1}) than in matrix ($\sim 10^{-7}$ cm^2 s^{-1}). Zero-order release kinetics were obtained for coated rings, and release rate decreases as the thickness of the coat increases. Cellulose membrane successfully eliminates burst release and controls the delivery from EVA rings. The equations developed can be used to determine the appropriate coat thickness to produce specific release rate.

KEY WORDS: burst release; cellulose membrane; drug delivery; intravaginal rings; progesterone.

INTRODUCTION

Polymeric matrix systems have been one of the most common types of devices in pharmaceutics and drug delivery applications. They present several advantages: low cost, easy fabrication, and less risk of dose dumping (2). In these systems, the drug or active pharmaceutical ingredient (API) is distributed through a polymeric phase that serves as diffusion barrier (3). The polymeric matrix can be nonporous (homogeneous) or porous (granular). If matrix is nonporous, it can be considered as one phase through which the drug diffuses. While, if matrix is porous, drug diffusion is restricted to pores in an otherwise impermeable material (4). API can be dissolved in the matrix or it can be dispersed in solid form. When the initial content is higher than drug solubility in the matrix, dissolved drug molecules co-exist with amorphous aggregates and/or drug crystals (known as monolithic dispersions).

Monolithic dispersions are commonly used in drug delivery field due to initial dose requirement. Drug release from monolithic dispersion systems is mainly controlled by diffusion process. Due to polymers' properties, swelling and/or erosion of polymeric matrix can also affect release rate (5–8). However, when the polymeric matrix does not degrade or swell in the liquid media, the release process is controlled mainly by the diffusion of solute through the matrix (9).

Controlled drug delivery systems are used to produce same therapeutic effect in patients than conventional dosage forms but with lesser amount of drug. The aim is to use the least amount of drug to produce the therapeutic action avoiding side effects. However, an initial large quantity of drug is released at early times when the device is a monolithic dispersions. In these systems, a high release is observed before it reaches a stable profile. This phenomenon is typically referred to as "burst release" or "burst effect" (10).

Burst release has been observed in numerous matrix-type systems (11–14). Also, several authors correlated the properties of the devices with burst phenomena. For example, Huang *et al.* correlated the polymeric matrix porosity and drug distribution with the initial burst release in poly(lactic-co-glycolic acid) (PLGA) microspheres (15). Duncan *et al.* studied the relationship between the solubility of the encapsulated protein and burst release in microspheres (16). Luan *et al.* indentified relevant parameters affecting the burst

[1] Laboratorio de Química Fina, Instituto de Desarrollo Tecnológico para la Industria Química (INTEC), Universidad Nacional del Litoral and Consejo Nacional de Investigaciones Científicas y Técnicas (UNL-CONICET), CCT CONICET-SANTA FE, Ruta Nacional 168, Paraje El Pozo, 3000, Santa Fe, Argentina.
[2] To whom correspondence should be addressed. (e-mail: ihelbling@santafe-conicet.gov.ar)

delivery of leuprolide acetate in PLGA microparticles (17). In addition, some efforts were made to describe the phenomena by mathematical models (10,18–20). A review has been published describing the causes of burst release and several mathematical models employed to study its role in controlled delivery devices (10).

Burst release is undesirable because release is uncontrollable during this stage. Also, high levels of API in patients can be harmful and increase the occurrence of undesired effects. In addition, the faster release observed during this period reduces the effective device lifetime. Several strategies have been proposed to overcome burst release. Hezaveh and Muhamad used genipin as crosslinker in kappa-carrageenan/polyvinyl alcohol hydrogels to reduce matrix swelling and hence release (21). Tan *et al.* coated nanogels with polyelectrolyte layers (22). Song *et al.* used a superhydrophobic coating in electrospun fibrous mat (23). Hasan *et al.* incorporated nanoparticles into microparticles to delay release (24). Several authors employed membranes of different polymers as coating for matrix-type device (25–27). An example of this is the commercial intravaginal ring Nuvaring® having a membrane of ethylene vinyl acetate copolymer (EVA) surrounding an EVA core (of different vinyl acetate content) impregnated with etonogestrel and ethinylestradiol (28). In summary, the goal of these strategies consists in delay the diffusion of the API through the polymeric device to reduce its delivery.

Contraception is a major concern in the modern woman. In breastfeeding women, contraception is provided by lactation amenorrhea. However, some patients desire an additional form of protection. For these cases, progestin-only contraceptives are preferable to estrogen-containing methods. Progestin-only contraceptives do not appear to affect milk volume, composition, or to cause deleterious effects in the infant (29). Progering® is a commercial progestin-only silicone ring releasing progesterone for contraception therapies during lactation. The ring releases the hormone by diffusion, maintaining a continuous flow of progesterone through the vaginal walls of about 10 mg day^{-1} (30). The progesterone induces the inhibition of the secretion of LH and FSH at the level of the hypothalamus and the pituitary, thereby inhibiting ovulation. It also has an effect on the cervical mucus making it more dense to prevent the penetration of sperm and inhibiting the proliferation of the endometrium. After the period of use, a new ring can be inserted if breastfeeding is continued and extended contraception is desired.

In our previous work, we fabricated a intravaginal ring made of EVA that contains progesterone (1). The ring is intended to deliver the hormone during 21 days for contraception purpose during lactation as an alternative to Progering®. After a period of 7 days without rings, a new device can be inserted. Results of our previous work show that the hormone was in solid state forming amorphous aggregates and drug crystals, and a lesser amount was presented as dissolved drug molecules inside EVA matrix (1). During the *in vitro* tests, a considerable burst release was observed. Approximately 20–40% of the hormone was released during burst phase (1). The objective of the present work is to evaluate the use of membranes to reduce or eliminate the burst release observed previously. For this goal, cellulose membranes were employed. In addition, the effect of membrane properties on hormone delivery was assessed using a mathematical model previously reported (31).

MATERIALS AND METHODS

Materials

Ethylene-vinyl acetate copolymer (EVA, vinyl acetate (VA) content of 28 wt%, Dupont®), progesterone (99.2%, Farmabase), and cellulose membrane (dialysis tubing cellulose membrane with a molecular weight cutoff of 12.4 KDa, Sigma-Aldrich®) were employed. All other reagents used were of analytical grade, except of methanol which was high-performance liquid chromatography (HPLC) grade. All aqueous solutions were prepared with ultra pure water.

Ring Preparation

Progesterone was incorporated into EVA pellets by an impregnation process (1,32). A known mass of progesterone was dissolved in dichloromethane and added to EVA pellets under agitation during 2 h. At this time, pellets swelled and absorbed all hormone solution. Then, pellets were dried to evaporate the organic solvent and precipitate the hormone inside pellets. This step was realized slowly to avoid higher efflux of solvent that could drag hormone out of pellets. Therefore, dried process was realized in vacuum at 40°C during 1 h and then in oven at 40°C until constant weight. Complete solvent evaporation was corroborated gravimetrically. Impregnated pellets were stored in a desiccator until ring fabrication.

EVA matrices containing progesterone were fabricated by hot-melt extrusion procedure using an industrial extruder (Dr. Collin® GmbH D-85560, Ebersberg). Impregnated pellets were fed into the extruder equipped with cylindrical die of several diameters, and the screw speed was set to 65 rpm. The temperature in the zones of feed, transport, compression, screened plate, and in the head was adjusted to 155°C, 160°C, 165°C, 170°C, and 175°C, respectively. All EVA extrudates were cooled down to room temperature and manually cut using surgical blades into matrices of specific length. A scheme of ring preparation from matrices is presented in Fig. 1a. Uncoated rings were fabricated placing the matrices onto stainless steel molds of required sizes, sealing matrix ends with heat at 170°C during approximately 1–2 min, and cooling down to room temperature. Coated rings were fabricated by a lab-scale batch processing. Dialysis tubings were cut longitudinal using a surgical blade to obtain cellulose membrane. The width of the membranes was adapted to the diameter of each matrix removing the excess of membrane with a scissor. Thereafter, membranes were attached to EVA matrices using medical grade acrylic adhesive. Coated matrices were placed onto stainless steel molds of required sizes and matrix ends were sealing with heat. After cooling down to room temperature, molds were closed for 30 min to ensure the joining of the membrane to the EVA matrix.

Rings were stored in a desiccator until their use. They were weighed and their dimensions were measured. The parameters R_e (outer radius of ring matrix) and R_0 (cross-

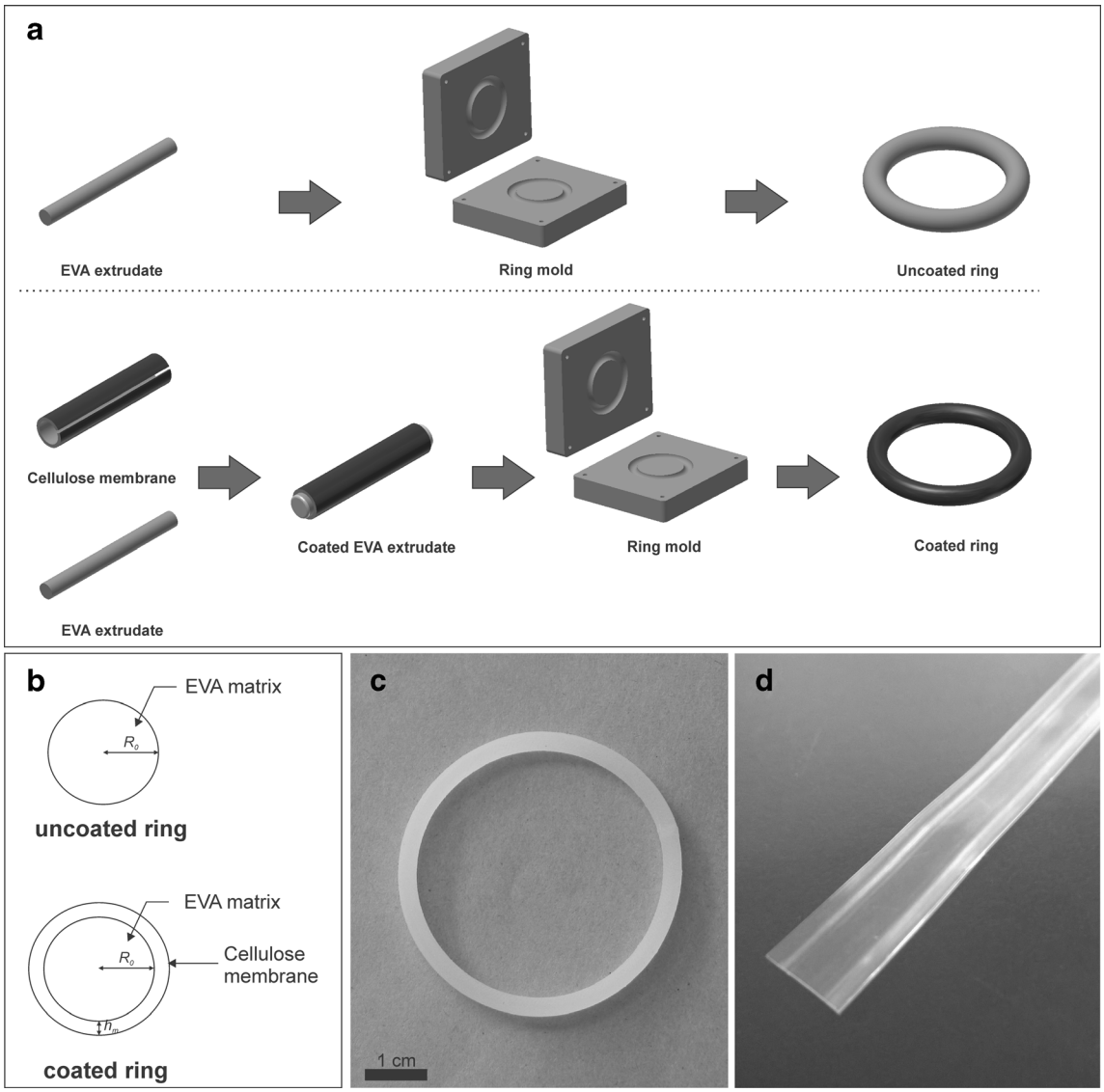

Fig. 1. EVA rings. **a** Ring preparation process from EVA matrices. **b** Scheme of cross-sectional view. **c** Coated ring with cellulose membrane. **d** Cellulose dialysis tubing

sectional radius of ring matrix) were calculated according to the technique reported in the bibliography (31). Ring density was also calculated. The hormone content in uncoated rings was determined extracting progesterone with 200 ml of ethanol in a Soxhlet during 48 h at 90°C. After a suitable dilution, progesterone concentration was measured by the HPLC technique detailed in "HPLC Determination of Progesterone" section and the initial amount of progesterone loaded (A) was calculated. In addition, the hormone content in coated rings was determined at several times of storage to analyze possible hormone migration to the membrane during ring storage. For that, rings were stored at room temperature during 7 days. At days 1, 3, and 7, membranes were detached from EVA matrix using a surgical blade and progesterone in each portion (matrix and membrane) was extracted with ethanol in a Soxhlet (experimental conditions similar to uncoated rings) and quantified by HPLC. All assay was run in triplicate.

Fourier Transform Infrared Spectroscopy (FTIR)

FTIR spectra of EVA and progesterone samples were recorded using a infrared spectroscopy (IR) spectrophotometer (FTIR-8201PC, Shimadzu) in the range of 400–4000 cm^{-1} with a 4-cm^{-1} resolution and 40 scans per spectrum.

Samples were prepared in the forms of potassium bromide (KBr) disk. To obtain a powder, impregnated and non-impregnated EVA rings were ground. Approximately 2 mg of sample (progesterone powder, EVA powder, and powder of EVA impregnated with the hormone) and 100 mg of KBr were dried at 30–40°C and 105°C, respectively, during 24 h. Powders were blended with a mortar, and the mixture was compacted using a IR hydraulic press at a pressure of 6 t for 3 min. The obtained disks were conditioned in a desiccator until measurements.

Differential Scanning Calorimetry (DSC)

EVA pellets and uncoated rings were analyzed by differential scanning calorimetry. Impregnated pellets, impregnated uncoated rings, and progesterone were also analyzed. Assays were carried out on a Mettler differential scanning calorimeter (TA 3000 with 30 DSC module, Mettler-Toledo). About 5 mg of samples was placed in an aluminum pan and heated at a rate of 10°C per min from −100°C to 200°C. An empty aluminum pan served as the inert control material. Nitrogen was used as purge gas.

EVA Intrinsic Viscosity and Molecular Weight

EVA solutions (0.002–0.006 g ml^{-1}) were prepared dissolving appropriate amounts of polymer in tetrahydrofuran (THF). The solvent and solution viscosity was measured in a thermostatized capillary viscometer at 23°C using a glass capillary tube no. 50. The intrinsic viscosity of EVA was determined plotting inherent and reduced viscosities *versus* solution concentration and extrapolating it to zero concentration (33). The EVA viscosity average molecular weight was calculated using the Mark-Houwink-Sakurada equation (34).

In Vitro Drug Release Assays

Progesterone release from uncoated and coated rings was studied using a Hanson Research SR8-Plus Dissolution Test Station (Hanson). Each ring was placed in 1000 ml of release medium, consisting of an hydroalcoholic medium with an ethanol content of 20% *v/v* and kept at 37°C and 100 rpm. Ethanol was added to enhance progesterone solubility in the medium (35). At different time points, aliquots of 5 ml were withdrawn and replaced with fresh medium to maintain a constant volume. The progesterone concentration in samples was measured by the HPLC technique detailed in "HPLC Determination of Progesterone" section. In addition, every 24 h, the entire volume was removed and replaced with fresh medium to maintain sink condition.

Scanning Electron Microscopy (SEM)

Internal morphology of impregnated rings was analyzed by scanning electron microscopy before and after the *in vitro* release assays. Samples were frozen and cryofractured under liquid nitrogen. Then, they were mounted on an aluminum holder and gold coated in an argon atmosphere in a 12157-AX sputter coater (SPI SUPPLIES) for 1 min to generate a thickness of 8 nm. Finally, samples were analyzed using a JSM-35C scanning electron microscope (JEOL) at an accelerating voltage of 20.0 kV.

Cellulose Membrane Characterization

Cellulose membranes were dipped in 10 ml of hydroalcoholic medium with ethanol content of 20% *v/v* during 5 min to achieve full hydration. Fully hydrated membranes were observed in an optical microscope (DM 2500M, Leica) with a coupled camera LEICA DFC 290 HD. Membrane thickness was measured in the photomicrographs using an image processing program.

Progesterone solubility in cellulose membranes was determined according to the technique reported by Wenhui (36). A saturated solution of progesterone was prepared dissolving 0.15 g of hormone in 150 ml of ultra filtered water. After weighed, the cellulose membranes were dipped in the saturated solutions and kept at 37°C in a Vicking M-23 shaker (Vicking) with a stirring speed of 100 rpm. Membranes were removed at different time (3, 4, and 5 weeks) to check if the equilibrium condition was reached. The hormone contained in each membrane was extracted with 200 ml of ethanol in a Soxhlet during 24 h at 90°C. After a suitable dilution, progesterone concentration was measured by the HPLC technique detailed in "HPLC Determination of Progesterone" section and the progesterone solubility in the membrane was calculated. The assay was run in triplicate. In addition, the partition coefficient between cellulose membrane and EVA matrix and cellulose membrane and release medium were calculated.

Progesterone diffusion coefficient in cellulose membrane was measured following the technique reported in the bibliography (36–39). A membrane was dipped in 10 ml of hydroalcoholic medium with an ethanol content of 20% *v/v* during 5 min to achieve full hydration. The fully hydrated membrane was placed between the donor and receptor compartment of a horizontal diffusion cells (Side-Bi-Side Cells). The surface area in which permeation occurs was $a_m = 1.7671$ cm^2. The donor compartment contains 5 ml of a saturated solution of progesterone containing a large excess of undissolved solute. Donor solution was prepared adding 0.5 g of progesterone in 10 ml of hydroalcoholic medium with an ethanol content of 20% *v/v*. The receptor compartment was filled with 5 ml of the hydroalcoholic medium. Both compartments were kept at 37°C under constant stirring. The total volume of receptor compartment (5 ml) was withdrawn at different times, and progesterone concentration was measured by the HPLC technique detailed in "HPLC Determination of Progesterone" section. The receptor compartment was filled with fresh medium to maintain sink condition. The assay was made in triplicate. The cumulative amount of hormone permeated was plotted *versus* time. The progesterone diffusion coefficient in the cellulose membrane (D_m) was calculated from the slope of the linear region of the curve (36–39).

HPLC Determination of Progesterone

Progesterone concentration in samples was analyzed by a HPLC system (Prominence LC20A, Shimadzu) equipped with a ZORBAX® Eclipse XDB-C_{18} column (5 μm particle size, 250 × 4.6 mm) at the wavelength of 254 nm (40). The mobile phase consisted of a mixture of HPLC grade methanol and ultra filtered water (95:5 *v/v*), and the flow rate was 1.0 ml min^{-1}. The column temperature was set to 30°C for all determinations. The progesterone elution time obtained in these condition was 3.7 ± 0.2 min.

Mathematical Modeling

The model reported in our previous work (31) was used to study and predict the *in vitro* release of progesterone from coated rings. Simulations were made using Matlab®. Theoretical predictions were compared with experimental data obtained during the *in vitro* assays. The f_1 and f_2 factors were used to measure quantitatively the fit of the model to the experimental data (41–43). The experimental data was selected as the reference profile, while the model prediction was chosen as the test profile. In addition, simulations were performed to analyze the influence of membrane properties over release rate.

RESULTS AND DISCUSSION

EVA Ring Fabrication

Figure 1a shows an illustration of the ring preparation process from EVA matrices, while Fig. 1b presents a scheme of the cross-sectional view of both types of rings. Both rings have similar appearance. They are flexible and have whitish color. Uncoated rings of different sizes were fabricated with cross-sectional radius equal to 0.15 ± 0.03, 0.17 ± 0.01, 0.30 ± 0.02, and 0.34 ± 0.01 cm. In addition, coated rings of four sizes were fabricated with cross-sectional radius equal to 0.194 ± 0.010, 0.214 ± 0.021, 0.344 ± 0.035, and 0.384 ± 0.028 cm (considering $R_0 + h_m$). A relationship between membrane thickness and matrix cross-sectional radius was defined as $\gamma = h_m/R_0$. For coated rings, experimental γ was 0.29, 0.26, 0.15, and 0.13, respectively. The matrix outer radius was $R_e = 2.27 \pm 0.03$ cm for all rings. Figure 1c presents an EVA ring coated with cellulose membrane, while Fig. 1d shows a cellulose dialysis tubing before their use. Cellulose membrane does not change ring appearance. No variation in flexibility was observed during membrane usage. In addition, the membrane successfully joined to the matrix. No separation of the two layers was detected during all release tests.

The initial content in uncoated rings was $A = 95.75 \pm 1.08$ mg cm^{-3}. For coated ring, hormone concentration in matrix and membrane zone was measured to analyze possible hormone migration. Progesterone concentration in matrix was 94.35 ± 2.08, 94.60 ± 1.50, 96.03 ± 2.10, and 95.22 ± 2.31 mg cm^{-3} for 0, 1, 3, and 7 days of storage at room temperature, respectively. The concentration in the membrane was 0, 0.54 ± 1.02, 0.32 ± 1.11, and 1.20 ± 1.13 mg cm^{-3} for days 0, 1, 3, and 7, respectively. As can be observed, progesterone was mainly distributed inside ring matrix. No progesterone particles were founded in the membrane at initial time. Hormone migration from matrix to membrane was negligible (<1.5% of initial content) during 7 days of storage. Further assays should be done to evaluate the occurrence of migrations at longer times.

Uncoated Rings

The intrinsic viscosity of EVA was 97.39 ± 0.59 cm^3 g^{-1}. The EVA viscosity average molecular weight was calculated using the Mark-Houwink-Sakurada equation (34). For the pair EVA and THF, the constant values are $K = 0.097$ cm^3 g^{-1} and $\alpha = 0.62$ (44). EVA viscosity average molecular weight was 69,425.7 g mol^{-1}.

FTIR was employed to study possible interaction between hormone and polymer. Figure 2 presents the results. In EVA spectra, it can be seen all the characteristic bands of the polymer functional groups: C–H bond in CH_3 groups at 2960 cm^{-1}, C=O bonds in acetyl groups at 1740 cm^{-1}, C–H bonds present in side chains at 1280 cm^{-1}, and C–O bonds in acetyl groups at 1040 cm^{-1}. The spectrum is similar to the data reported in the literature by other authors (45,46). Progesterone spectra also show all the molecule functional groups bands: C–H bond in methyl groups at 2960 cm^{-1}, C=O bonds in ketone groups at 1724 cm^{-1}, methyl group at 1375 cm^{-1}, and methyl-ketone group at 1354 cm^{-1}. These spectra are similar to that reported in the literature (47,48). Finally, uncoated ring spectrum shows all the characteristic bands of the polymer and the hormone. No additional band was observed. From spectra comparison, no chemical interaction between the hormone and the polymer was detected.

DSC analyses are commonly used to provide information about thermal properties of samples and physicochemical state of active principles inside polymeric matrices (49–51). Figure 3 presents DSC analysis results for EVA and progesterone samples. In pellet samples (see Fig. 3a), glass transition temperature (T_g) of EVA was observed at around −30°C. These results are in agreement with values reported in the literature (52,53). EVA melting endotherm was quite complex and wide, starting at around 30°C and 40°C for pellet and pellet impregnated with progesterone, respectively, and ending approximately at 90°C for both. Results are in

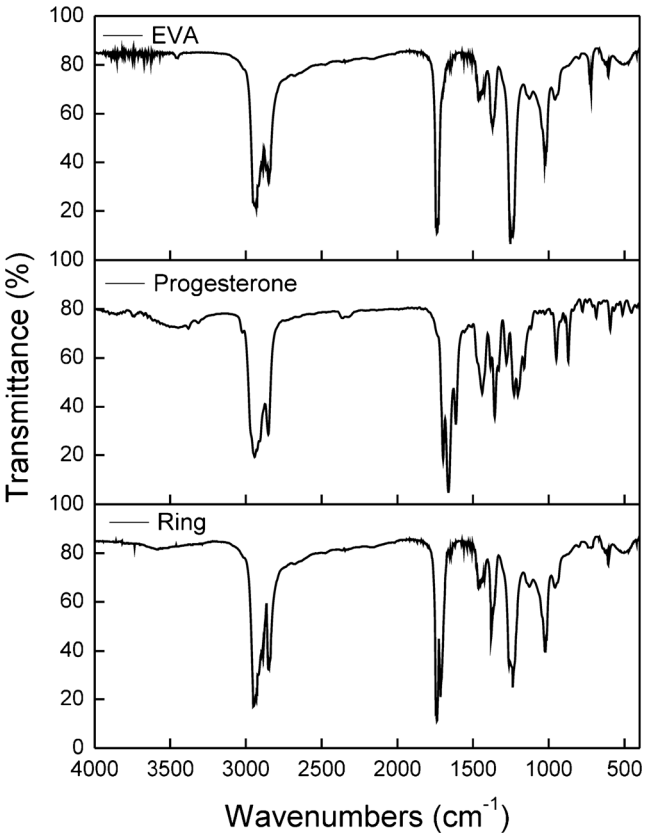

Fig. 2. FTIR spectra of EVA, progesterone, and uncoated rings

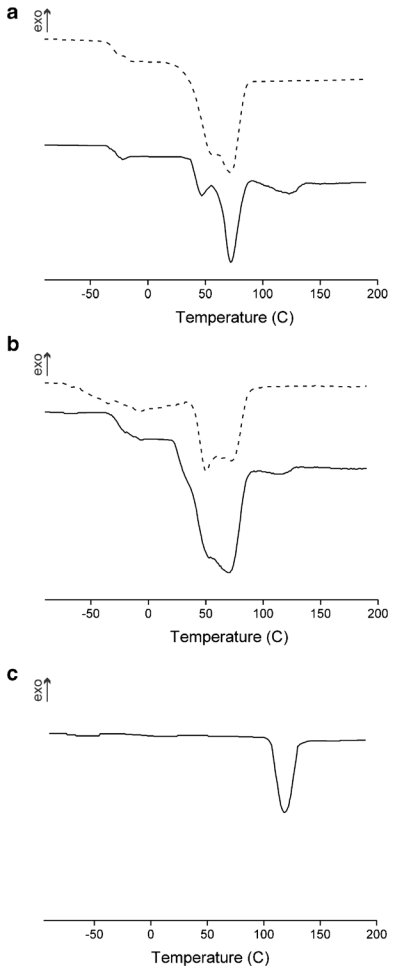

Fig. 3. DSC analysis. **a** Pellets (*broken line*). Pellets impregnated with progesterone (*straight line*). **b** Rings (*broken line*). Rings impregnated with progesterone (*straight line*). **c** Progesterone (*straight line*)

agreement with those reported by other authors (52–54). These wide endotherms would indicate the presence of a large continuum of crystal morphologies and sizes. EVA copolymer is composed of poly ethylene (PE) groups and VA groups. PE is the only crystallisable comonomer in EVA copolymer. The melting temperature for pure PE is 120°C. VA is polar, non-crystalline (amorphous) and perturbs the crystallization of perfect PE crystals. This creates a complex crystalline organization inside polymer structure. In EVA pellets, a main wide endothermic peak is observed suggesting a continuum crystal morphologies. However, in pellets impregnated with the hormone, two major components can be distinguished corresponding to the presence of two predominant crystal morphologies. One component at low temperature (endothermic peak at around 45°C) due to less perfect crystals and a second one at higher temperature (endothermic peak at around 72°C) corresponding to crystals of the best organized PE chains in the copolymer. These results would suggest that impregnation process could alter EVA structure and crystallinity. During organic solvent removal, less perfect crystal formation could be favored which was reflected by the presence of the endothermic peak at around 45°C. Finally, a broad endothermic peak corresponding to progesterone crystals melting was observed in the range of 100–135°C for pellets impregnated with the hormone. Only crystalline state of drugs can be detected by DSC analysis. It has been reported that no detectable endotherm is produced when the drug is in a molecular dispersion or a solid solution state (49). Progesterone has two polymorphs, form I (α-form) and form II (β-form) (48,55). Form I (thermodynamically more stable form) has melting point at 128°C, whereas form II has melting endotherm at 122°C (55,56).

In ring samples (see Fig. 3b), EVA glass transition temperature was also observed at around −30°C. The EVA melting endotherm appears in the range of 40–90°C and 25–90°C for EVA rings and progesterone-impregnated EVA rings, respectively. In both cases, a continuum crystal morphology is suggested. During ring fabrication, temperature was set to 155–175°C. This leads to polymer and drug melting. Thereafter, rapid cooling to room temperature and the storage at room temperature induce crystal formation in the polymer (room temperature is between the melting and glass transition temperatures of EVA). Hence, crystals of several sizes and morphologies were formed during ring storage. This fact is reflected in the broad endothermic peak observed for both samples. Finally, a small peak was noted around 100–130°C corresponding to progesterone crystals melting for hormone-containing rings. No endothermic peak was observed in that zone for rings that do not contain the hormone.

In progesterone samples (see Fig. 3c), an endothermic peak corresponding to hormone crystal melting is observed at about 110–130°C. This result is in agreement with the range reported by other authors (55,56). As can be noted, endothermic peak for progesterone sample is higher than the corresponding peak for the hormone in pellet and ring samples. DSC spectra comparisons would suggest that only a small amount of hormone is present as crystals form in the pellets and rings. In these samples, progesterone is mostly in amorphous state. This could be attributed to dissolution/precipitation and melting/solidification process that take place during impregnation and hot-melt extrusion procedure, respectively.

Figure 4 presents the *in vitro* release of progesterone from EVA rings of different sizes. The hormone is distributed in the matrix, and the diffusion of dissolved drug is the controlling step. Therefore, typical matrix-type release profiles are expected: a high mass of solute was released at initial time (burst release) followed by a rapidly declining of the release rate with time. As rings have different sizes, release was normalized dividing the amount released by the area of each ring. Delivery was assayed during 21 days since this is the expected period of use. From the figure, the release kinetics seems to be of first order for all devices. Also, a considerable burst release was noted at early times. These results are in agreement with those observed in our previous work (1). In addition, the effect of matrix cross-sectional diameter on delivery was studied. Rings with $R_0 = 0.15$ cm and $R_0 = 0.17$ cm reached a plateau at around day 4, meaning that at this day all the hormone was released. For rings with higher R_0, the plateau was reached at around day 14. These results show that rising cross-sectional diameter of matrix leads to an increase of device lifetime.

Figure 5 shows the morphology of uncoated EVA ring before and after *in vitro* release assays. It was reported that

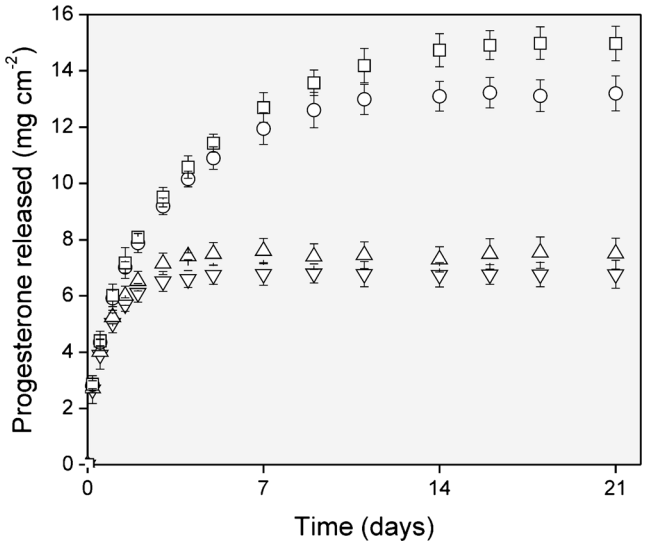

Fig. 4. *In vitro* release of progesterone from uncoated rings. Symbols: *white down-pointing triangle*: $R_0 = 0.15$ cm; *white down-pointing triangle*: $R_0 = 0.17$ cm; *white circle*: $R_0 = 0.30$ cm; *white square*: $R_0 = 0.34$ cm

the state of progesterone inside matrix depends on the amount loaded (57). As the initial content of progesterone in the EVA rings was higher than hormone solubility in the polymeric matrix, dispersed particles co-exist together with dissolved particles. Dispersed particles can aggregate forming bigger structures that are embedded into the matrix phase. It was reported that melting of progesterone followed by a rapid cooling produces agglomerates (48). During a study of polymorphs of progesterone, melting and rapid cooling led to the formation of irregular agglomerates of the hormone that were broken under the force of ultrasonication (48). Figure 5a shows agglomerates of progesterone inside EVA matrix. This aggregates could be formed during the hot-melt extrusion procedure wherein melting and rapid cooling occur. During delivery assays, release medium penetrates EVA matrix and the drugs present in the aggregates dissolve in and diffuse out of rings creating "holes." These holes can be observed in Fig. 5b.

In summary, the large amount of progesterone released at early times during the *in vitro* tests can be explained by the following reasons: (i) no chemical interactions that delayed drug release could be detected between drug and polymer; (ii) most of the hormones are forming irregular amorphous aggregates inside rings which could be dissolved easier than crystalline form in the liquid medium; and (iv) the hormone is markedly smaller than polymer. Hence, dissolved molecules of progesterone could diffuse easily through polymer matrix.

In our previous work, we evaluated the *in vitro* delivery in several release medium and we found that in 20% *v*/*v* of ethanol, the EVA rings do not swell or degrade and the release is controlled by progesterone diffusion through EVA matrix (1). In addition, the entire release medium was replaced to maintain sink conditions. These conditions are similar to those that occurred *in vivo* in the vaginal cavity: rings do not swell or degrade, release is diffusion-controlled, and sink condition is maintained during the therapy. For these reasons, we chose this solution as release medium. However, it is important to point out that release rate obtained *in vitro* is not a measure of *in vivo* release rate. *In vivo* performance needs to be addressed. Issues like tissue-material partitioning, vaginal fluid volume, mixing/permeability of the surrounding environment with devices, and absorption rate through vaginal mucosa affect *in vivo* release leading to differences with data observed *in vitro*. It is inferred that *in vivo* delivery could be lesser than *in vitro* due to the smaller volume of vaginal fluids compared to the 1000 ml of *in vitro* release medium, but burst phase is also expected *in vivo*. Pharmacokinetic studies should be performed in order to determine the effect of these issues.

Coated Rings

As was observed, uncoated rings presented a considerable burst release during first hours. In most of applications, burst release is undesirable. A common strategy to overcome this problem is the use of membranes covering the matrix. Membranes delay interaction between solute contained in the matrix and release medium and at the same time control solvent penetration time, solute diffusion, and delivery rate (25–27).

Cellulose membranes were characterized. Fully hydrated cellulose membranes were observed in a microscope and the average thickness was $h_m = 0.044 \pm 0.004$ cm. Progesterone solubility in the membrane was determined at three times of storage. Figure 6a presents the solubility in the units of mass

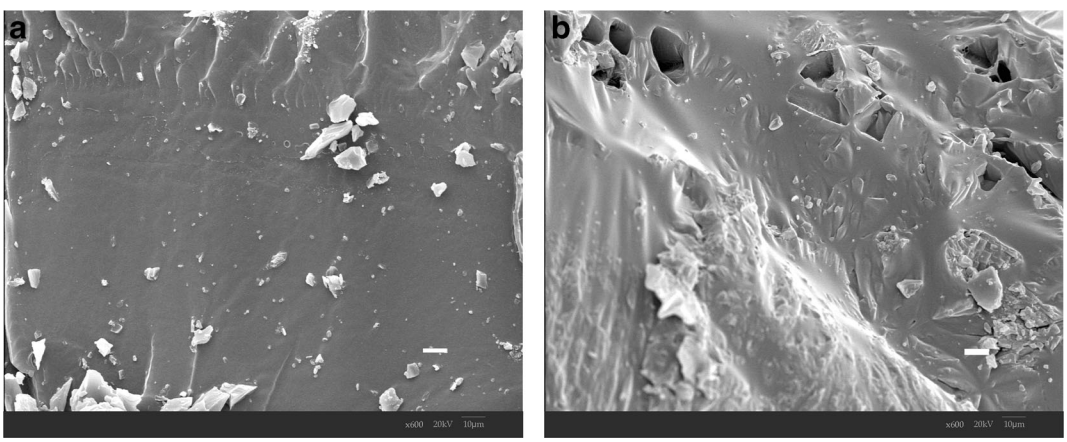

Fig. 5. Internal morphology of uncoated EVA rings. **a** Before release assays. **b** After release assays

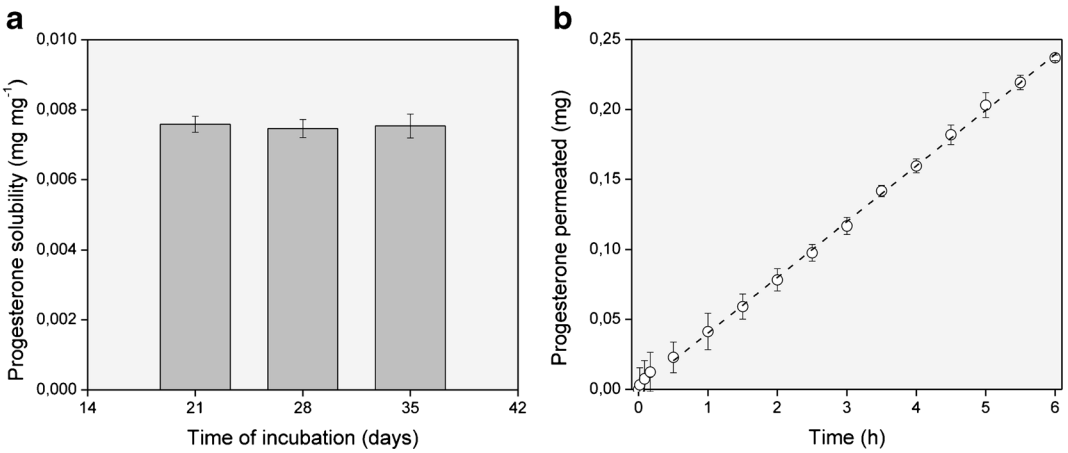

Fig. 6. Characterization of cellulose membrane. **a** Progesterone solubility. **b** Progesterone permeation assay: *white circle*: experimental data; *broken line*: pseudo-steady state fit

of progesterone per mass of cellulose membrane at different times. As can be observed, the content of hormone in each membrane was very similar suggesting that the equilibrium condition was reached at 21 days. The average solubility was $C_p = 12.59 \pm 0.15$ mg cm^{-3}. Progesterone solubilities in EVA matrix and in the hydroalcoholic medium were reported previously (1). These values are $C_s = 25.39 \pm 3.01$ mg cm^{-3} and $C_a = 0.18 \pm 0.01$ mg cm^{-3}, respectively (1). With these data, partition coefficients were calculated. The partition coefficient between cellulose membrane and EVA matrix was $K_2 = 0.4958$, while the partition coefficient between release medium and cellulose membrane was $K_3 = 0.0143$.

Progesterone diffusion coefficient in the cellulose membrane was determined in permeation assays.

Results are presented in Fig. 6b. Two stages can be observed: an initial stage with high permeation rate and then a second stage in which steady state is reached and permeation rate remains approximately constant. Similar behavior for other solutes were reported in the bibliography (20). The high permeation rate observed during the first instants could be attributed to the small thickness of membranes and the high surface/volume ratio, which promotes a large initial permeation of hormone (20). Then, steady state was reached at approximately 30 min from the beginning of the test. A linear fit was done with steady state experimental data, and determination coefficient $R^2 = 0.999$ was obtained. The progesterone diffusion coefficient (D_m) was calculated from the linear fit using the following equation (36–39):

$$\frac{\partial m}{\partial t} = \frac{D_m C_a a_m}{K_3 h_m} \quad (1)$$

in which $\partial m/\partial t$ is the slope of the steady state linear fit, C_a is the progesterone solubility in the donor solution, $K_3 = C_a/C_p$ is the partition coefficient between the donor solution and the membrane, a_m is membrane area in which permeation occurs, and h_m is membrane thickness. A value of dm/dt = 0.0398 mg h^{-1} was obtained from the fitting. The membrane area was $a_m = 1.7671$ cm^2. Using these data and the values of h_m, C_a, and K_3 previously determined, the progesterone diffusion coefficient in the cellulose membrane was $D_m = (2.22 \pm 0.17) \times 10^{-8}$ cm^2 s^{-1}. Progesterone diffusion coefficient in EVA matrix was determined in our previous work, and it is $D_p = (1.05 \pm 0.04) \times 10^{-7}$ cm^2 s^{-1} (1). These values suggest that the hormone diffuses more slowly through the cellulose membrane than through the EVA matrix. Hence, cellulose membrane could be used to control the delivery from EVA rings.

Progesterone delivery from coated rings was studied, and released profiles are presented in Fig. 7a. As rings have different sizes, release was normalized dividing the amount released by the area of each ring. Delivery was assayed during 21 days since this is the expected period of use. It can be seen that the use of cellulose membranes covering EVA matrix markedly modifies release kinetic comparing with uncoated rings. Burst release was eliminated and a lag time was observed at early instants during which no hormone was released. Lag time corresponds to time required for solvent penetration through membrane, dissolution of the hormone present in the outer layer of the matrix, and dissolved drug diffusion through membrane to reach release medium bulk. Thereafter, amount of progesterone released slightly rises with time reaching a steady state during which release rate remains relatively constant generating zero-order kinetics. This result is consistent with those reported in the literature (25–27). Rings with $R_0 = 0.15$ cm and $R_0 = 0.17$ cm released progesterone with zero-order kinetics during around 11 days. Thereafter, a decrease in delivery rate is observed which could be due to the fact that matrix is about to deplete. For the rings with higher R_0, the zero-order kinetics was maintained for 21 days. As in uncoated rings, the rise in cross-sectional diameter of matrix leads to an increase of device lifetime.

For comparison purposes, the release during the first 5 h from uncoated and coated rings is presented in Fig. 7b. The first 5 h were taken arbitrarily as a measure of the burst release. For uncoated rings, the percentage released was $37.21 \pm 3.96\%$, $33.34 \pm 2.15\%$, $19.82 \pm 2.56\%$, and $17.61 \pm 1.98\%$ for $R_0 = 0.15$, 0.17, 0.30, and 0.34 cm, respectively (the corresponding release per unit area was 2.67 ± 0.51, 2.71 ± 0.12, 2.85 ± 0.14, and 2.87 ± 0.34 mg cm^{-2}, respectively). For coated rings, the percentage released was $0.04 \pm 0.89\%$, 0.07

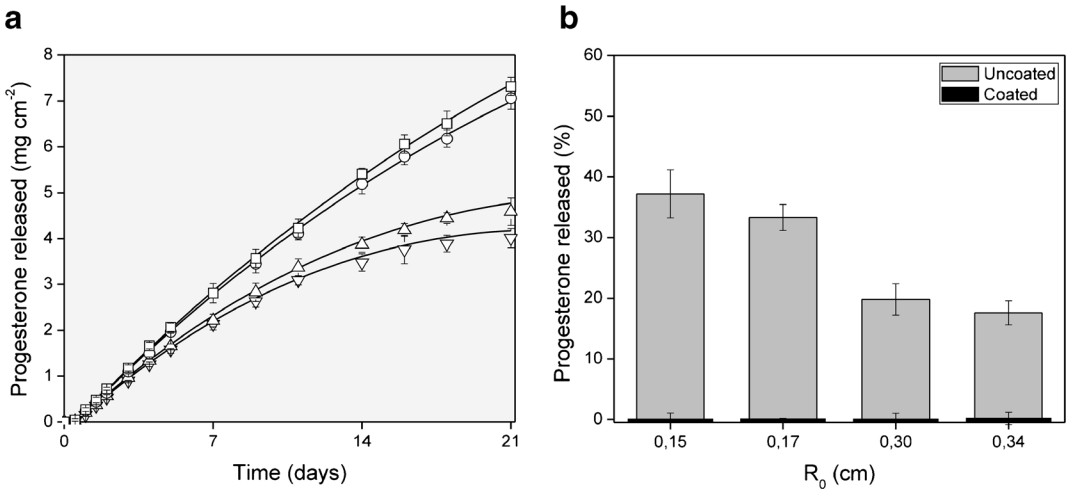

Fig. 7. Progesterone delivery. **a** Progesterone released from coated rings. Symbols: *white down-pointing triangle*: $R_0 = 0.15$ cm; *white up-pointing triangle*: $R_0 = 0.17$ cm; *white circle*: $R_0 = 0.30$ cm; *white square*: $R_0 = 0.34$ cm; *straight line*: theoretical prediction of Eq. (2). **b** Comparison of progesterone released at 5 h

$\pm 0.64\%$, $0.03 \pm 0.71\%$, and $0.17 \pm 0.55\%$ for $R_0 = 0.15$, 0.17, 0.30, and 0.34 cm, respectively. Coated rings delivered lesser amount of hormone than uncoated rings and the percentage delivered at 5 h was negligible suggesting that burst release was eliminated. In addition, the effect of matrix cross-sectional diameter on delivery was studied. The percentage of hormone delivered decreases with an increment of R_0 because as R_0 rises, device size also rises and higher mass of hormone is available to be released. Hence, the mass released at specific time is lesser compared to the total mass available as device size increases. In conclusion, the use of cellulose membrane was efficient in the reduction/elimination of burst release. Also, membranes successfully controlled progesterone release from rings. This could be due mainly to the smaller diffusion coefficient of the hormone in the membrane ($\sim 10^{-8}$ cm^2 s^{-1}) compared with that in the matrix ($\sim 10^{-7}$ cm^2 s^{-1}). As in uncoated rings, *in vitro* release rate from coated rings is not a measure of *in vivo* delivery. But the elimination of burst phase *in vitro* is a positive result suggesting that similar burst reduction could be expected in the vaginal cavity. Pharmacokinetic studies should be performed in order to determine *in vivo* release rate needed to provide contraceptive efficacy and systemic levels that do not induce undesired effects. As reference, Progering® delivers the progesterone through the vaginal walls at about 10 mg day^{-1} (30).

Drug delivery from coated rings can be study with the model developed in our previous work (31). The cumulative amount of drug released in a given time can be calculated with the following equation (31):

$$m = 2\pi^2 R_g \left[A\left(R_0^2 - (S - R_g)^2\right) + \frac{C_s S(S-2R_g)\ln\left(\frac{(R_g+S)R_e}{S(R_g+R_e)}\right) - (C_s - C_{eq,2})\left(R_g(R_e - S) + 3R_g{}^2\ln\left(\frac{R_g+S}{R_g+R_s}\right)\right)}{\ln\left(\frac{(R_g+S)R_e}{S(R_g+R_e)}\right)} - C_{eq,2}R_e(R_e - 2R_g)(1-K_2) - \frac{C_{eq,2}K_2\left(R_g h_m + 3R_g{}^2\ln\left(\frac{R_g+R_e}{R_g+R_e+h_m}\right)\right)}{\ln\left(\frac{(R_g+R_e)(R_e+h_m)}{R_e(R_g+R_e+h_m)}\right)} \right] \quad (2)$$

where m is the cumulative amount of drug released, R_g is the distance from rotation axis to the center of the generating circle of ring matrix, A is the initial load of drug in the device, R_0 is ring matrix cross-sectional radio, S is the position of the dissolution–diffusion moving front, C_s is drug solubility in matrix, R_e is outer radius of ring matrix, $C_{eq,2}$ is dissolved drug concentration in matrix at the matrix-membrane interface, K_2 is drug partition coefficient at the matrix-membrane interface and h_m is membrane thickness (31). The position of the "dissolution–diffusion moving front" (S) can be obtained with the follow implicit expression (31):

$$\frac{R_e(R_g+R_e)-S(R_g+S)}{6}+\frac{{R_g}^2}{6}\ln\left(\frac{R_g+S}{R_g+R_e}\right)-\left(\frac{S^3}{3R_g}+\frac{S^2}{2}\right)\ln\left(\frac{(R_g+S)R_e}{S(R_g+R_e)}\right)+$$
$$\frac{D_p}{D_m K_2}\ln\left(\frac{(R_g+R_e)(R_e+h_m)}{R_e(R_g+R_e+h_m)}\right)\left(\frac{({R_e}^3-S^3)}{3R_g}+\frac{({R_e}^2-S^2)}{2}\right)=\frac{D_p t}{\left(\frac{A}{C_s}-1\right)} \quad (3)$$

where t is time and D_p and D_m are drug diffusion coefficient in matrix and membrane, respectively (31). Equations (2) and (2) were employed to study drug delivery from coated rings. Figure 7a presents simulation results. The following parameter values were used in the predictions: $A = 95.75 \pm 1.08$ mg cm^{-3}; $C_s = 25.39 \pm 3.01$ mg cm^{-3} (1); $R_e = 2.27 \pm 0.03$ cm; $R_0 = 0.15 \pm 0.03$, 0.17 ± 0.01, 0.30 ± 0.02, and 0.34 ± 0.01 cm; $D_p = (1.05 \pm 0.04) \times 10^{-7}$ cm^2 s^{-1} (1); $K_2 = 0.4958$; $h_m = 0.044 \pm 0.004$ cm; and $D_m = (2.22 \pm 0.17) \times 10^{-8}$ cm^2 s^{-1}. As can be observed, the model seems to adequately predict the experimental data.

In order to measure quantitatively the fit of the model to the experimental data, the f_1 and f_2 factors were used. The f_1 measures the percent error between two curves over all time points while f_2 is a logarithmic transformation of the sum-squared error of differences between both curves over all time points. The procedure for calculating these factors was reported in the literature (41–43). The f_1 is zero when test and reference profiles are identical and increases proportionally with the dissimilarity between them. The f_2 is 100 when the test and reference profiles are identical and tends to 0 as the dissimilarity increases. In general, f_1 values lower than 15 (0–15) and f_2 values higher than 50 (50–100) show the similarity between profiles (41–43). Factor f_1 was 5.27, 2.98, 3.90, and 4.09 for coated rings with matrix cross-sectional diameter of 3.0, 3.4, 6.0, and 6.8 mm, respectively, while f_2 was 99.99, 100.00, 99.99, and 99.99 respectively. Therefore, theoretical and experimental profiles can be considered similar for all devices. Based on this rigorous quantitative analysis, it can be concluded that the model previously developed predicts satisfactorily the experimental release profiles obtained in the *in vitro* assays for coated rings.

As cellulose membrane successfully controlled hormone delivery from EVA rings, the effect of membrane thickness over release was studied using the mathematical model. Results are shown in Fig. 8. For theoretical prediction, the follows parameter values were used: $A = 95.75 \pm 1.08$ mg cm^{-3}, $C_s = 25.39 \pm 3.01$ mg cm^{-3}, $R_0 = 0.30 \pm 0.02$ cm, $R_e = 2.27 \pm 0.03$ cm, $D_p = (1.05 \pm 0.04) \times 10^{-7}$ cm^2 s^{-1}, $K_2 = 0.4958$, and $D_m = (2.22 \pm 0.17) \times 10^{-8}$ cm^2 s^{-1}. Figure 8a presents the fraction of drug released over time for coated rings with membranes of different sizes. As h_m increases, γ increases and the fraction of drug released decreases. This was expected since the membrane delays drug release in several ways. As membrane thickness increases, liquid media need more time to take contact with drug particles. In addition, drug particles must diffuse higher distances to be released out of the device. Therefore, these phenomena lead to a decrease in the fraction of drug released at a given time as γ increases.

Figure 8b presents dissolved drug concentration profiles at specific time point (five days of release) for different values of γ. In the figure, X is the dimensionless spatial coordinate along cross-sectional radius of ring and θ is the dimensionless dissolved drug concentration, defined by:

$$X = r - R_g \quad \theta = \frac{C}{C_s} \quad (4)$$

where r is dimensional spatial coordinate along cross-sectional radius of rings and C is dimensional dissolved drug concentration. A value of $X = 0$ ($r = R_g$) represents the midpoint of ring matrix cross-sectional diameter and $X = 0.30$ ($r = R_0$) corresponds to the matrix surface. Values of $X > 0.30$ ($r > R_0$) correspond to the membrane. Similarly, $\theta = 0$ ($C = 0$) is zero concentration of dissolved drug while $\theta = 1$ ($C = C_s$) represents dissolved drug concentration equal to drug solubility in matrix. Three regions can be observed in all profiles: (I) dispersed drug zone, (II) depletion zone, and (III) membrane. In the dispersed drug zone, moving front cannot enter yet in contact with solid drug aggregates and

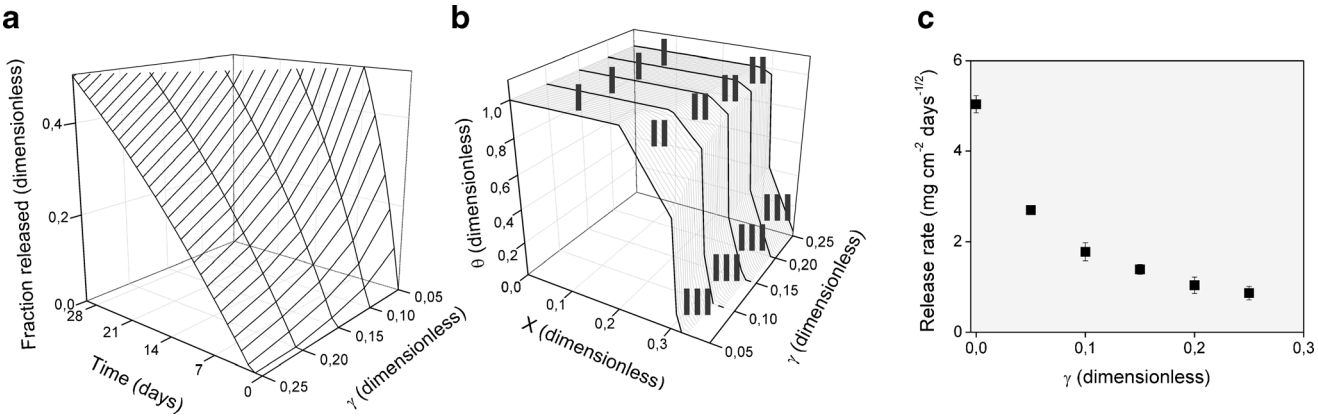

Fig. 8. Effect of membrane thickness over release. **a** Fraction of drug released. **b** Dissolved-drug concentration profiles after 5 days of release. **c** Release rate

hence the amount of drug in dissolved state is equal to drug solubility in matrix (because this is the initial amount of dissolved drug contained in the matrix). This is represented by $\theta = 1$. In the depletion zone, moving front dissolved all solute particles. Therefore, no dispersed drug is presented. The dimensionless position of the dissolution-diffusion front (δ) at a particular time is denoted by the interface between dispersed drug zone and depletion zone. Dissolved drug particles diffuse out of device generating a linear concentration gradient between moving front position and matrix surface. At matrix surface, a partition phenomena exists due to difference in matrix and membrane drug solubility. Finally, a linear concentration gradient of dissolved drug is observed in the membrane. As h_m increases (γ increases), moving front required more time to reach the matrix. Thus, when h_m is small, moving front is closer to the midpoint of matrix ring cross-sectional diameter (more close to $X = 0$), while for high h_m values, moving front is in matrix surface proximity. This suggests that membrane delays the liquid media inlet to the matrix and hence reduces the release.

Figure 8c presents release rate of coated rings for different values of γ. An increment in membrane thickness leads to a decrease in release rate. As mentioned before, membranes with higher thickness delay contact between liquid medium and solid drug particles increase diffusion distance to reach release medium and therefore decrease the mass of solute released diminishing release rate. Varying membrane thickness, different release rate can be obtained. Equations (1) and (2) can be used to find the appropriate coat thickness to produce a specific release rate required for an application.

CONCLUSIONS

Matrix-type devices usually present first-order kinetics during *in vitro* assays. This type of release implies the existence of burst effect at short times. Burst effect is undesirable in many application due to the risk associated with high levels of drug and uncontrollable delivery. A known strategy to eliminate burst effect is the use of membranes to coat the polymeric matrix. In this context, cellulose membranes were used to cover ring-shaped EVA matrices. Uncoated rings presented typical first-order release profiles with high burst release at initial instants. Contrary, coated rings presented no burst effect. The use of these membranes successfully controls the release rate from EVA rings, allowing to achieve zero-order release kinetics up to release of about 60–65% of total drug load. Modifying membrane thickness, release rate can be adjusted to a specific required value. As membrane thickness increases, the contact between liquid medium and solid drug aggregates is delayed. In addition, diffusion distance to reach release medium increases. These together lead to a diminishing in the mass of drug released and in the corresponding release rate. Equations (1) and (2) can be used to find the appropriate coat thickness to produce a specific release rate required.

Cellulose membranes are suitable for release control from EVA rings due to their properties: a hydrophobic nature similar to EVA, good hormone solubility, and a diffusion coefficient smaller than that corresponding to EVA matrix. As can be observed in the results, progesterone diffusion coefficient in cellulose membrane ($\sim 10^{-8}$ cm^2 s^{-1}) is one order of magnitude smaller than in EVA matrix ($\sim 10^{-7}$ cm^2 s^{-1}). This allows the membrane to control hormone release. It is important to note that all results presented in this contribution were obtained *in vitro*. Pharmacokinetic studies should be performed in order to determine ring performance in the vaginal cavity.

ACKNOWLEDGMENTS

The authors wish to express their gratitude to Consejo Nacional de Investigaciones Científicas y Técnicas (CONICET) and to Universidad Nacional del Litoral (UNL) of Argentine, for the financial support granted to this contribution.

REFERENCES

1. Helbling I, Ibarra JD, Luna J. The optimization of an intravaginal ring releasing progesterone using a mathematical model. Pharm Res. 2014;31(3):795–808.
2. Siepmann J, Siepmann F. Mathematical modeling of drug delivery. Int J Pharm. 2008;364(2):328–43.
3. Wen H, Park K. Introduction and overview of oral controlled release formulation design. Oral controlled release formulation design and drug delivery: John Wiley & Sons, Inc.; 2010. p. 1–19.
4. Frenning G. Modelling drug release from inert matrix systems: from moving-boundary to continuous-field descriptions. Int J Pharm. 2011;418(1):88–99.
5. Göpferich A. Mechanisms of polymer degradation and erosion. Biomaterials. 1996;17(2):103–14.
6. Lee PI. Modeling of drug release from matrix systems involving moving boundaries: approximate analytical solutions. Int J Pharm. 2011;418(1):18–27.
7. Colombo P. Swelling-controlled release in hydrogel matrices for oral route. Adv Drug Deliv Rev. 1993;11(1–2):37–57.
8. Colombo P, Bettini R, Massimo G, Catellani PL, Santi P, Peppas NA. Drug diffusion front movement is important in drug release control from swellable matrix tablets. J Pharm Sci. 1995;84(8):991–7.
9. Zhou Y, Wu XY. Finite element analysis of diffusional drug release from complex matrix systems. I. Complex geometries and composite structures. J Control Release. 1997;49(2):277–88.
10. Huang X, Brazel CS. On the importance and mechanisms of burst release in matrix-controlled drug delivery systems. J Control Release. 2001;73(2–3):121–36.
11. Kishida A, Murakami K, Goto H, Akashi M, Kubota H, Endo T. Polymer drugs and polymeric drugs X: slow release of 5-fluorouracil from biodegradable poly(γ-glutamic acid) and its benzyl ester matrices. J Bioact Compat Polym. 1998;13(4):270–8.
12. Atkins TW, Tighe BJ, McCallion RL. Incorporation and release of fluorescein isothiocyanate-linked dextrans from a bead-formed macroporous hydrophilic matrix with potential for sustained release. Biomaterials. 1993;14(1):16–20.
13. Vasudev SC, Chandy T, Sharma CP. Development of chitosan/polyethylene vinyl acetate co-matrix: controlled release of aspirin-heparin for preventing cardiovascular thrombosis. Biomaterials. 1997;18(5):375–81.
14. Messaritaki A, Black SJ, van der Walle CF, Rigby SP. NMR and confocal microscopy studies of the mechanisms of burst drug release from PLGA microspheres. J Control Release. 2005;108(2–3):271–81.
15. Huang X, Li N, Wang D, Luo Y, Wu Z, Guo Z, *et al.* Quantitative three-dimensional analysis of poly (lactic-co-glycolic acid) microsphere using hard X-ray nano-tomography revealed correlation between structural parameters and drug burst release. J Pharm Biomed Anal. 2015;112:43–9.

16. Duncan G, Jess TJ, Mohamed F, Price NC, Kelly SM, van der Walle CF. The influence of protein solubilisation, conformation and size on the burst release from poly(lactide-co-glycolide) microspheres. J Control Release. 2005;110(1):34–48.
17. Luan X, Skupin M, Siepmann J, Bodmeier R. Key parameters affecting the initial release (burst) and encapsulation efficiency of peptide-containing poly(lactide-co-glycolide) microparticles. Int J Pharm. 2006;324(2):168–75.
18. Bruschi ML. Mathematical models of drug release, strategies to modify the drug release from pharmaceutical systems. Woodhead Publishing; 2015. p. 63–86.
19. Xiang A, McHugh AJ. Quantifying sustained release kinetics from a polymer matrix including burst effects. J Membr Sci. 2011;371(1–2):211–8.
20. Narasimhan B, Langer R. Zero-order release of micro and macromolecules from polymeric devices: the role of the burst effect. J Control Release. 1997;47:13–20.
21. Hezaveh H, Muhamad II. Controlled drug release via minimization of burst release in pH-response kappa-carrageenan/polyvinyl alcohol hydrogels. Chem Eng Res Des. 2013;91(3):508–19.
22. Tan JPK, Wang Q, Tam KC. Control of burst release from nanogels via layer by layer assembly. J Control Release. 2008;128(3):248–54.
23. Song B, Xu S, Shi S, Jia P, Xu Q, Hu G, *et al*. Superhydrophobic coating to delay drug release from drug-loaded electrospun fibrous materials. Appl Surf Sci. 2015;359:245–51.
24. Hasan AS, Socha M, Lamprecht A, Ghazouani FE, Sapin A, Hoffman M, *et al*. Effect of the microencapsulation of nanoparticles on the reduction of burst release. Int J Pharm. 2007;344(1–2):53–61.
25. Charalambopoulou GC, Kikkinides ES, Papadokostaki KG, Stubos AK, Papaioannou AT. Numerical and experimental investigation of the diffusional release of a dispersed solute from polymeric multilaminate matrices. J Control Release. 2001;70(3):309–19.
26. Georgiadis MC, Kostoglou M. On the optimization of drug release from multi-laminated polymer matrix devices. J Control Release. 2001;77(3):273–85.
27. Bodmeier R, Paeratakul O. Drug release from laminated polymeric films prepared from aqueous latexes. J Pharm Sci. 1990;79:32–6.
28. Roumen FJ, Dieben TO. Clinical acceptability of an ethylene-vinyl-acetate nonmedicated vaginal ring. Contraception. 1999;59(1):59–62.
29. Kelsey JJ. Hormonal contraception and lactation. J Hum Lact. 1996;12(4):315–8.
30. Brache V, Payan LJ, Faundes A. Current status of contraceptive vaginal rings. Contraception. 2013;87(3):264–72.
31. Helbling IM, Luna JA, Cabrera MI. Mathematical modeling of drug delivery from torus-shaped single-layer devices. J Control Release. 2011;149:258–63.
32. Helbling IM, Ibarra JCD, Luna JA. Evaluation and optimization of progesterone release from intravaginal rings using response surface methodology. J Drug Delivery Sci Technol. 2015;29:218–25.
33. ASTM International. ASTM D2857, Standard practice for dilute solution viscosity of polymers. 2001.
34. Kurata M, Tsunashima Y. Viscosity-molecular weight relationships and unperturbed dimensions of linear chain molecules. 3rd edn ed. New York, USA.: John Wiley and Sons; 1989.
35. Bunt CR, Rathbone MJ, Burggraaf S, Ogle CR. Development of a QC release assessment method for a physically large veterinary product containing a highly water insoluble drug and the effect of formulation variables upon release. Proc Int Symp Control Release Bioact Mater. 1997;24:145–6.
36. Wenhui D. Mechanism of diffusion of progesterone through ethylene vinyl acetate copolymer. J China Pharmaceutical Univ. 1987;18:87–90.
37. Barry BW. Dermatological formulations: percutaneous absorption. New York, USA: Marcel Dekker; 1983.
38. Paul DR, McSpadden SK. Diffusional release of a solute from a polymeric matrix. J Memb Sci. 1976;1:33–48.
39. Flynn GL. Physicochemical determinants of skin absorption. Gerrity TR, and Henry, C. J., editor. New York, USA: Elsevier; 1990.
40. Pereira GR, Marchetti JM, Bentley MVLB. A rapid method for determination of progesterone by reversed-phase liquid chromatography from aqueous media. Anal Lett. 2000;33:881–9.
41. Costa P, Sousa Lobo JM. Modeling and comparison of dissolution profiles. Eur J Pharm Sci. 2001;13:123–33.
42. Moore JW, Flanner HH. Mathematical comparison of dissolution profiles. Pharm Technol. 1996;20:64–74.
43. Pillay V, Fassihi R. Evaluation and comparison of dissolution data derived from different modified release dosage forms: an alternative method. J Control Release. 1998;55:45–55.
44. Mori S, Barth HG. Size exclusion chromatography. Alemania: Springer; 1999.
45. Tang M, Hou J, Lei L, Liu X, Guo S, Wang Z, *et al*. Preparation, characterization and properties of partially hydrolyzed ethylene vinyl acetate copolymer films for controlled drug release. Int J Pharm. 2010;400(1–2):66–73.
46. Zhu Y, Otsubo M, Honda C. Degradation of polymeric materials exposed to corona discharges. Polym Test. 2006;25:313–7.
47. Sjahfirdi L, Septian A, Maheshwari H, Astuti P, Suyatna FD, Nasikin M. Determination of estrous period in female rats (Rattus norvegicus) by Fourier transform infrared (FTIR) through identification of reproductive hormones in blood samples. World Appl Sci J. 2011;14(4):539–45.
48. Tripathi R, Biradar SV, Mishra B, Paradkar AR. Study of polymorphs of progesterone by novel melt sonocrystallization technique: a technical note. AAPS Pharm Sci Technol. 2010;11(3):1493–8.
49. Mu L, Feng SS. Fabrication, characterization and *in vitro* release of paclitaxel (Taxol) loaded poly (lactic-co-glycolic acid) microspheres prepared by spray drying technique with lipid/cholesterol emulsifiers. J Control Release. 2001;76(3):239–54.
50. Dubernet C. Thermo analysis of microspheres. Thermochim Acta. 1995;248:259–69.
51. Gupte A, Ciftci K. Formulation and characterization of Paclitaxel, 5-FU and Paclitaxel + 5-FU microspheres. Int J Pharm. 2004;276(1–2):93–106.
52. Bai Y, Qian J, An Q, Zhu Z, Zhang P. Pervaporation characteristics of ethylene–vinyl acetate copolymer membranes with different composition for recovery of ethyl acetate from aqueous solution. J Membr Sci. 2007;305(1–2):152–9.
53. Bistac S, Kunemann P, Schultz J. Crystalline modifications of ethylene-vinyl acetate copolymers induced by a tensile drawing: effect of the molecular weight. Polymer. 1998;39(20):4875–81.
54. Meng FH, Schricker SR, Brantley WA, Mendel DA, Rashid RG, Fields Jr HW, *et al*. Differential scanning calorimetry (DSC) and temperature-modulated DSC study of three mouthguard materials. Dent Mater. 2007;23(12):1492–9.
55. Duclos R, Saiter JM, Grenet J, Orecchioni AM. Polymorphism of progesterone. J Therm Anal. 1991;37(8):1869–75.
56. Muramatsu M, Iwahashi M, Takeuchi U. Thermodynamic relationship between α- and β-forms of crystalline progesterone. J Pharm Sci. 1979;68(2):175–7.
57. Hill VL, Paserini N, Craig DQM, Vickers M, Anwar J, Feely LC. Investigation of progesterone loaded poly(d, l-lactide) microspheres using TMDCS, SEM and PXRD. J Therm Anal. 1998;54:673–85.